

## Elastic and thermal properties of heat-resistant steels and nickel-based alloys

Anatoly Rinkevich, Natalia Stepanova, Dmitry Rodionov

Institute of Metal Physics Ural Division of the RAS, 18 S.Kovalevskaya St, Ekaterinburg, 620219 Russia, rin@imp.uran.ru

Modern techniques need creation of the heat-resistant single crystal materials. Among them the greatest prospects have the steel single crystals and also the alloys on nickel basis. The heat-resistant nickel alloys are applied to blade manufacturing in the stationary and aviation gas-turbine engines. The single crystals 60N21 could be considered as a convenient modeling object. In the given work comparison between elastic and thermal characteristics of 60N21 steel is carried out. Besides, attention is paid to the single crystal samples of  $\text{Ni}_3(\text{Al-Nb})$  alloy and of some heat-resistant nickel alloys. The measurements of elastic wave velocities in several crystallographic directions have been carried out. The components of elasticity moduli tensor are designed on the velocity values. The Debye temperature that is an important parameter for estimation thermal properties of an alloy is calculated using known values of moduli. There is a distinct correlation between the factor of anisotropy of a crystal and the Debye temperature. The purpose of research was not only reception of numerical values of these characteristics, but also comparison of these values to a fraction of the strengthening  $\gamma'$ -phase. Distribution of the acoustic fields has been investigated in the 60N21 steel in different structural states, namely austenitic single crystal, martensitic pseudo-single crystal, austenitic polycrystal. Symmetry of the acoustic beam and the local peculiarities of the ultrasonic field also are studied. The attenuation coefficient and the magnetic field dependence of ultrasound velocity are measured.

### 1 Introduction

Heat-resistant steel single crystals and alloys on nickel basis work in conditions of heats and in excited environment [1]. For this group of alloys the  $\text{Ni}_3\text{Al}$  intermetallic compound is base in which there are temperature anomalies of the deformation characteristics, and also the effect of thermal hardening connected to them. It is known, that high elastic anisotropy renders the most essential influence on the temperature dependence of ultimate strength [2]. Therefore a lot of experimental works has been devoted to measuring of elastic moduli of the  $\text{Ni}_3\text{Al}$  single crystals in a wide temperature range [2-5].

The steel single crystals also represent perspective objects of research of elastic properties [6]. By present time only individual works by definition of elasticity moduli of steel single crystals are performed by ultrasonic methods [7]. At the same time studying of moduli and other physical characteristics has the practical importance [6]. The 60N21 steel single crystals could be considered as a convenient modeling object. Its elastic properties were studied in [8,9], and a special attention was given to the kind of acoustic fields in various structural conditions. In the given work comparison between the elastic and thermal characteristics of the 60N21 steel is carried out.

Certain researches are performed on the single crystal samples of the  $\text{Ni}_3(\text{Al-Nb})$  alloy and of some heat-resistant nickel alloys. In the first case the samples

were single-phase ( $\gamma'$ -phase), in the second case they were two-phase alloys ( $\gamma$  solid solution on the basis of nickel and intermetallic  $\gamma'$ -phase). The volume fraction of the intermetallic phase varied in the investigated alloys over a wide range. Measurements of the elastic wave velocities in several crystallographic directions were carried out. The components of elasticity moduli tensor were designed on the velocity values. Further the shear modulus  $G$  and the bulk modulus  $B$  have been determined, and the factor of anisotropy  $A$  was designed. The Debye temperature that is an important parameter for estimation thermal properties of an alloy was calculated using known values of moduli. The purpose of research was not only reception of numerical values of these characteristics, but also comparison of these values to a fraction of strengthening  $\gamma'$ -phase.

### 2 Experimental methods

At first let's consider characteristics of the samples used in the work. A steel single crystal with composition: C (0,59 %); Ni (20,9 %); Mn (0,57 %); Si (0,3 %) is grown by Bridgemen method. The single crystal was approximately cylindrical in shape 22mm in diameter. It was in austenitic paramagnetic state and had the cellular grown structure with the characteristic dimensions of the order of  $0.2\pm 0.5\text{mm}$ . Length of the sample, that is a distance between two parallel planes,

a normal to which in limits  $\pm 2^0$  coincided with the [110] direction, is equal 0.788 cm.

The contents of  $\gamma$ -phase in the investigated nickel alloys varied from 5 volume percent for the EI-437B alloy up to 67 % for the ZhS-36alloy. The TsNK-8MP alloy is assigned to corrosion-resistant. In an alloy of VKNA-type the volume fraction of intermetallic phase is increased up to 95 %. In a single crystal sample of an alloy with composition 75 % Ni - 19 % Al - 6 % Nb a volume fraction of  $\gamma$ -phase achieves practically 100 %. Deviation of normal to a sample plane from crystallographic axes  $\langle 001 \rangle$ ,  $\langle 110 \rangle$  or  $\langle 111 \rangle$  did not exceed  $1^0 - 3^0$ . Thickness of the samples made 4 - 10 mm. The ultrasonic measurements are executed by an echo-method. Measurements were made on shear waves with the frequency of 5 MHz and on longitudinal waves with the frequency of 5 and 15 MHz. The error of velocity measurement makes no

more than 0,5 %. Two samples of each material have been investigated for alloys on a nickel basis. In one sample the propagation direction has been chosen along an axis  $\langle 100 \rangle$ , in the another along an axis  $\langle 110 \rangle$  or  $\langle 111 \rangle$ . Measurements on shear waves at the propagation direction  $\langle 110 \rangle$  are carried out for two eigenmodes. Polarization directions of these eigenmodes are  $u // [100]$  and  $u // [1 \bar{1} 0]$ .

### 3 Elastic velocities and moduli

The results of the ultrasonic measurements are shown in Table 1. The values of velocities measured in km/s are collected in Table 1. The propagation direction is specified by a wave vector  $q$ .

Table 1. Elastic wave velocities

Alloy	Longitudinal waves			Shear waves			
	$q // [100]$	$q // [110]$	$q // [111]$	$q // [100]$	$q // [110]$		$q // [111]$
					$u // [100]$	$u // [1 \bar{1} 0]$	
60N21		5.59			3.73	2.09	
EI-437B	5.45		6.50	3.84			2.93
TsNK-8MP casted	5.46	6.28		4.03	3.97	2.37	
TsNK-8MP annealed	5.48	6.30		3.94	4.03	2.35	
ZhS-36	5.36	6.18		3.88	3.78	2.29	
VKNA	5.08	6.04		3.75	3.78	2.21	
Ni <sub>3</sub> (Nb, Al)	5.56	6.42		4.08	4.04	2.34	

On the values of velocities it is possible to calculate components of the elastic moduli tensor of single crystals [10]. For a propagation direction [100] connection of moduli with velocities of waves is expressed by formulas

$$\rho s_{L[100]}^2 = c_{11}; \rho s_{T[100]}^2 = c_{44}, \quad (1)$$

where  $\rho$  is the density,  $s_{L[100]}$  and  $s_{T[100]}$  the phase velocities of longitudinal (L) and shear (T) waves with a propagation direction [100]. For a propagation direction [111] the similar formulas look as follows

$$\begin{aligned} \rho s_{L[111]}^2 &= 1/3(c_{11} + 2c_{12} + 4c_{44}); \\ \rho s_{T[111]}^2 &= 1/3(c_{11} + c_{44} - 2c_{12}), \end{aligned} \quad (2)$$

where for velocities of waves the similar designations are entered at a propagation direction [111]. In a direction [110] two eigenmodes propagate and the formulas connecting moduli and velocities of waves may be written as

$$\begin{aligned} \rho s_{L[110]}^2 &= 1/2(c_{11} + c_{12} + 2c_{44}); \\ \rho s_{T1[110]}^2 &= c_{44}, \rho s_{T2[110]}^2 = 1/2(c_{11} - c_{12}), \end{aligned} \quad (3)$$

where the shear wave with polarization along [100] is designated by the index T1, and the wave with polarization along  $[1 \bar{1} 0]$  by the index T2. For calculation of the module  $c_{12}$  the following formulas were used

$$c_{12} = \rho (s_{L[110]}^2 - s_{T1[110]}^2 - s_{T2[110]}^2). \quad (4)$$

$$c_{12} = \rho (s_{L[100]}^2 + s_{T[100]}^2 - 3s_{T[111]}^2). \quad (5)$$

The results received for the moduli are listed in Table 2. In the same place on the references for comparison

the values of the elastic moduli components for the intermetallic compound Ni<sub>3</sub>Al are shown.

Table 2. Elastic module, density and Debye temperature

Alloy	Elastic module, GN/m <sup>2</sup>			Density, kg/m <sup>3</sup>	Debye temperature, K
	C <sub>11</sub>	C <sub>12</sub>	C <sub>44</sub>		
60N21	172	102	110	7.9	428
EI-437B	234	149	116	7.87	465
TsNk-8MP casted	252	140	137	8.46	471
TsNk-8MP annealed	254	152	131	8.46	472
ZhS-36	249	152	130	8.65	447
VKNA	215	145	117	8.35	382
Ni <sub>3</sub> (Nb, Al)	240	141	129	7.75	467
Ni <sub>3</sub> Al	223 [2]	148 [2]	125 [2]	7.56	462 [4]

### 4 The Debye temperature

The Debye temperature  $T_D$  is entered as a limiting frequency in an oscillation spectrum of a solid. The Debye temperature can be defined from the elastic module values [11] using a method offered by Leibfried. Within the framework of this method calculation  $T_D$  is conducted following to the formula

$$T_D = \frac{h}{k} \left( \frac{3N}{4\pi V} \right)^{1/3} \left( \frac{c_{11} - c_{44}}{\rho} \right)^{1/2} J, \tag{6}$$

where  $h$  is the Planck's constant,  $k$  the Boltzman constant,  $N/V$  the number of atoms in unit of volume, and quantity  $J$  could be calculated depending on parameters

$$C = \frac{c_{44}}{c_{11} - c_{44}} = \frac{A}{2}, \quad K = \frac{c_{12} + c_{44}}{c_{11} - c_{44}}. \tag{7}$$

Results of calculation of the Debye temperature are presented in Table 2. The attention that fact pays to itself, that the Debye temperature for the VKNA single crystal is appreciably less then for other materials.

It is essential, that parameter  $C$  in the formula (7) is proportional to the factor of anisotropy  $A$  for a cubic crystal. Therefore, using the method designed by Leibfried, it is possible to try to check up presence of a correlation between the elastic anisotropy and the thermal characteristics of a material. About an opportunity of such correlation in heat - resistant alloys it was spoken in [2]. The results of calculation of the factor of anisotropy  $A$  are shown in Table 3. On Figure 1 the alloys are located in ascending order the factor of

anisotropy from the cast TzNK-8MP with the least factor  $A = 2,42$  up to the VKNA alloy with a very great value  $A = 3,34$ . On an ordinate axis in Figure 1 the values of the Debye temperature are plotted.

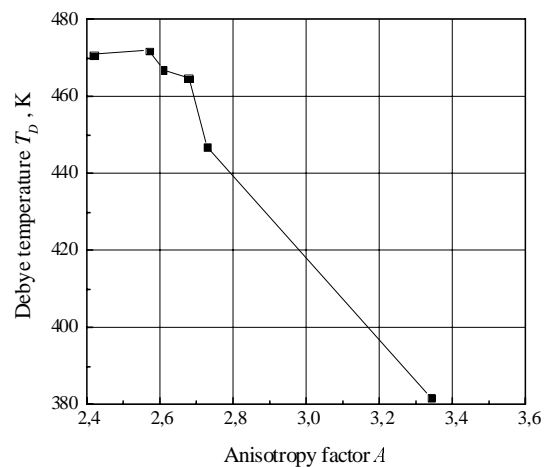


Figure 1. Correlation between the factor of elastic anisotropy and Debye temperature in heat - resistant alloys on a nickel basis

A distinct correlation is evident: with increase of anisotropy of a crystal the Debye temperature goes down. The value of the anisotropy factor  $A$ , certain by us for the VKNA alloy, coincides with the value for Ni<sub>3</sub>Al from [2]:  $A=3,34$ . From elastic moduli received the tensor components resulted in Table 3, have been designed the bulk module  $B$  and the shear module  $G$ . For calculation the relations are used

$$B = \frac{c_{11} + 2c_{12}}{3}, \quad G = \frac{G_V + G_R}{2}, \quad (5)$$

$$G_V = \frac{c_{11} - c_{12} + 3c_{44}}{5}, \quad G_R = \frac{5(c_{11} - c_{12})c_{44}}{4c_{44} + 3(c_{11} - c_{12})}$$

$G_V$  (the top border of an estimation of modulus  $G$ ). The results of calculations are shown in Table 3.

where an "isotropic" modulus  $G$  is introduced as average between the modulus  $G_R$  (that is the bottom border of an estimation of modulus  $G$ ) and the modulus

Table 3. Elastic moduli  $B$  and  $G$  and anisotropy factor of alloys

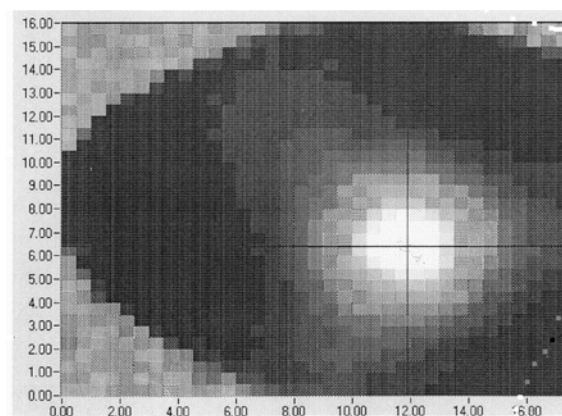
Alloy	Anisotropy factor	Modulus $B$ , GN/m <sup>2</sup>	Modulus $G_V$ , GN/m <sup>2</sup>	Modulus $G_R$ , GN/m <sup>2</sup>	Modulus $G$ , GN/m <sup>2</sup>	Relation $B/G$
EI-437B	2.73	1.77	0.87	0.69	0.78	2.28
TzNK-8MP casted	2.42	1.77	1.05	0.87	0.96	1.85
ZhS-36	2.68	1.84	0.97	0.78	0.88	2.10
VKNA	3.34	1.68	0.84	0.60	0.74	2.27
Ni <sub>3</sub> (Nb, Al)	2.61	1.74	0.97	0.79	0.88	1.98

## 5 Acoustic fields

Visualization of acoustic fields has become an effective method of investigation of elastic anisotropy and internal material structure. View of acoustic fields in polycrystal and multiphase materials allows to estimate the elastic nonhomogeneity degree and to discover the main sources of the elastic waves scattering. Using the acoustic field it is convenient to study the elastic anisotropy and homogeneity in single crystals. The acoustic fields in a steel single crystal have been studied in [8] by the laser interferometric method. The aim of this paper is to investigate thoroughly the elastic fields in 60N21 steel when the sample is at first an austenitic single crystal, then it becomes a martensitic pseudo-single crystal after  $\gamma \rightarrow \alpha$ -transformation and at last an austenitic polycrystal after reversal  $\alpha \rightarrow \gamma$ -transformation. The internal structure was carefully elaborated in every state with optical and transmission electron microscopy. The OFV-3000S interferometer brought about the laser detection of ultrasound.

The results of the acoustic field investigation in the steel single crystal are shown in Figure 2 as a C-type scan. Measurements are carried out on the longitudinal waves at the frequency  $f = 10$  MHz when the ultrasonic wave vector is directed along the [111] crystal axis,  $q \parallel [111]$ . The digits along the X- and Y- axes represent the distance in mm from the starting point of scanning. The lines connecting the points (X=0.00; Y=10.5) and (X=7.50; Y=16.0) as well as (X=0.0; Y=6.5) and (X=7.0; Y=0) restrict the plane part of the sample. The center of the transducer's projection is marked by the

cross section of the horizontal and vertical lines. Brightness represents the amplitude of the oscillations in the picture: maximal amplitude corresponds to the light spot. The amplitude distribution in the central part of the beam is axially symmetrical whereas the peripheral part reflects the three-fold symmetry. The beam is expanded along the  $\langle 112 \rangle$ -type directions. That clearly seen symmetry of the beam is a consequence of strong elastic anisotropy influence of the austenitic single crystal on the ultrasound



propagation.

Figure 2. Longitudinal wave acoustic field in the steel single crystal detected by the laser interferometer

## 6 Magnetic field dependence

The cooling of the sample in liquid nitrogen and its exposure at the temperature of  $T=-196^{\circ}\text{C}$  for 5 min was fulfilled in order to transform the sample from an austenitic into a martensitic state. At least 90% of martensite was originated in the sample as a result of  $\gamma\rightarrow\alpha$ -transformation and the single crystal had converted in a pseudo-single crystal. Sharp nonhomogeneity of the acoustic energy distribution should be mentioned for the martensitic state, with a nonhomogeneity size varying over the wide limits from 0.125mm (that is a resolution of the installation) to  $\sim 8\text{mm}$ . Based on the metallographic analysis of the structural heterogeneities dimensions in the austenitic and martensitic states and comparing these dimensions with the ultrasonic wavelength one can make the following conclusion. The nonhomogeneity of the acoustic fields in the martensitic state is caused mainly by the scattering on the martensitic structure formed inside the growth cells of the initial austenitic single crystal. Austenitic polycrystal structure was obtained when the sample was slowly heated with the speed of 5 degrees per minute at first to  $780^{\circ}$ , and then to  $1000^{\circ}\text{C}$  (that is  $\gamma$ -region) with 15 minutes exposure. After the exposure the sample was air-cooled to room temperature. The grains of two morphological types originate in  $\gamma$ -region: globular in shape with  $3-8\mu$  in size and elongated look like martensitic grains of  $\gamma$ -phase with the length up to  $20-30\mu$  and the width  $\sim 3\mu$ . Investigation with the electron transmission microscope shown that both the separate carbide particles are in the structure and the cementite-type carbide chains of the  $(\text{Fe Ni})_3\text{C}$ . The elastic energy distribution has the usual type for the polycrystal structure.

The magnetic field dependence of the longitudinal wave velocity is plotted in Figure 3 at the frequency of 50 MHz. Magnetic field is directed perpendicularly to the propagation direction. The curve I related to the martensitic state shows the velocity at first increases, then saturates and even a bit decreases in high fields. The dependencies obtained for the austenitic state after heating up to  $780^{\circ}\text{C}$  and  $1000^{\circ}\text{C}$ , are practically equal each other (curves II and III). The ultrasonic velocity in the austenitic state decreases monotonically without saturation when the magnetic field intensity increases. The carbides influence on the attenuation coefficient. Measuring the magnetization the decrease of the ferromagnetic carbides volume from 0,7% to 0,2% was ascertained after the additional heating to  $1000^{\circ}\text{C}$ . The attenuation coefficient decreased, too. Therefore, the contribution in attenuation ( $\sim 3,5\text{ dB/cm}$  at 50 MHz) occurs stipulated by scattering on the carbide particles and on the carbide chains especially. Notice that the size of separated carbide particles is not so important for the scattering in the Raleigh region, but the size of the

austenitic grains around which the chains are located plays a dominant role. In our experiment the discussed contribution is observed under such condition when the averaged austenitic grain sizes are substantially lower than the ultrasonic wavelength.

By and large the detailed analysis is carried out of the acoustic signals and the magnetic field dependencies of the velocity of ultrasound and attenuation coefficient for the austenitic and martensitic states. The latter measurements show that the carbide chains are very important for ultrasonic scattering at the frequencies about dozens of megahertz.

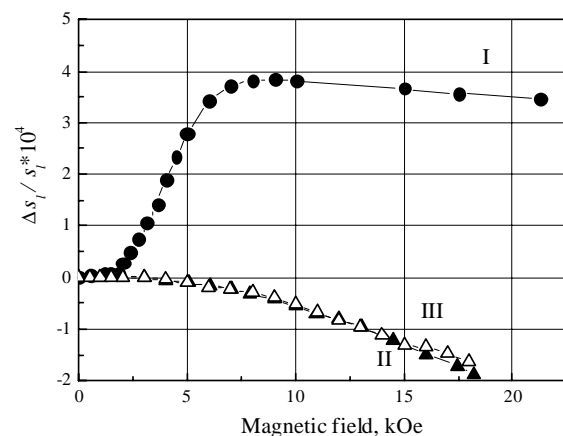


Fig.3. Magnetic field dependence of the longitudinal wave velocity measured at 50 MHz for the martensitic and austenitic states

## 7 Summary

In summary we shall note, that in this work the velocities of elastic waves have been measured in a 60N21 steel single crystal and its elasticity tensor has been restored. The factor of anisotropy which appeared one of the biggest for cubic crystals of transition metals is determined. The Debye temperature values are determined. Acoustic research of elastic properties of some heat - resistant nickel alloys (EI-437B, TzNK8-MP, ZhS-36, VKNA) is carried out. Components of elastic moduli tensor are obtained. The values of the factor of anisotropy are determined and the Debye temperature values are obtained by Leibfried method. There is a distinct correlation between the factor of anisotropy of a crystal and the Debye temperature.

## References

- [1] N.S.Stoloff, Physical and mechanical metallurgy of  $\text{Ni}_3\text{Al}$  and its alloys, *Internation. Mater. Rev.*, Vol.34. N 4. pp.153-184. (1989)
- [2] M.H.Yoo, High-temperature ordered intermetallic alloys, ed. N.S. Stoloff et. al., *MRS Symposia Proc.*, Pittsburgh, N 81. pp.207. (1987)
- [3] R.W.Dicson, J.B.Wachtman, Elastic constants of single crystal  $\text{Ni}_3\text{Al}$  from  $10^\circ$  to  $850^\circ\text{C}$ , *J.Appl. Phys.*, Vol. 40. N5. Pp.2276-2279. (1969)
- [4] K.Ono, R.Stern, Elastic constants of  $\text{Ni}_3\text{Al}$  between  $80^\circ$  and  $600^\circ\text{K}$ , *Trans. Met. Soc. AIME*, Vol.245. N2. pp.171-172. (1969)
- [5] F.X.Kayser, C.Stassis, The elastic constants of  $\text{Ni}_3\text{Al}$  at 0 and  $23.5^\circ\text{C}$ , *Phys. Status Solidi*, Vol.64. pp.335. (1981)
- [6] D.P.Rodionov, V.M.Schatlivtsev, *Steel single crystals*, Ekaterinburg,, 274 p. (1996) (in Russian)
- [7] H.M.Ledbetter, Predicted single-crystal elastic constants of stainless steel 316, *Brit. J. of NDT*. Vol.23. N6. pp.286-287. (1981)
- [8] A.B.Rinkevich, A.M.Burkhanov, D.P.Rodionov, Yu.V.Khlebnikova, B.Koehler, Acoustic fields in a steel single crystal in austenitic and martensitic states, *Phys.Met. and Metallography*, V.92. N3. pp.240-250. (2001)
- [9] A.M.Burkhanov, A.B.Rinkevich, D.P.Rodionov, Elasticity moduli and the Debye temperature of single crystal steel 60H21, *Phys.Met. and Metallography*, Vol.93.N6. Pp.563-566. (2002)
- [10] R.Truell, Ch.Elbaum, B.Chick. *Ultrasonic methods in solid state physics*, N.Y.: Academic Press, 307 p. 1969
- [11] Physical acoustics, ed. W.P.Mason, V.III, part B. *Lattice dynamics*, N.Y.: Academic Press, 391 p. 1965